

Occludin is required for TRPV1-modulated paracellular permeability in the submandibular gland

Xin Cong¹, Yan Zhang¹, Ning-Yan Yang², Jing Li², Chong Ding³, Qian-Wen Ding⁴, Yun-Chao Su¹, Mei Mei², Xiao-Hong Guo¹, Li-Ling Wu^{1,*} and Guang-Yan Yu^{2,*}

¹Center for Salivary Gland Diseases of Peking University School and Hospital of Stomatology, Department of Physiology and Pathophysiology, School of Basic Medical Sciences, Peking University Health Science Center and Key Laboratory of Molecular Cardiovascular Sciences, Ministry of Education, Beijing, China

²Department of Oral and Maxillofacial Surgery, Peking University School and Hospital of Stomatology, Beijing, China

³Central Laboratory, Peking University School and Hospital of Stomatology, Beijing, China

⁴Department of Dental Emergency, Beijing Stomatological Hospital, Capital Medical University, Beijing, China

*Authors for correspondence (pathophy@bjmu.edu.cn; gyyu@263.net)

Accepted 17 December 2012

Journal of Cell Science 126, 1109–1121

© 2013. Published by The Company of Biologists Ltd

doi: 10.1242/jcs.111781

Summary

Occludin plays an important role in maintaining tight junction barrier function in many types of epithelia. We previously reported that activation of transient receptor potential vanilloid subtype 1 (TRPV1) in rabbit submandibular gland promoted salivary secretion, partly by an increase in paracellular permeability. We have now explored the role of occludin in TRPV1-modulated paracellular permeability in a rat submandibular gland cell line SMG-C6. Both TRPV1 and occludin were expressed in SMG-C6 cells, and capsaicin induced redistribution of occludin, but not claudin-3, claudin-4 or E-cadherin, from the cell membrane into the cytoplasm. Capsaicin also decreased transepithelial electrical resistance (TER) and increased the Trypan Blue and FITC-dextran flux. Capsazepine (CPZ), a TRPV1 antagonist, inhibited the capsaicin-induced occludin redistribution and TER decrease. Moreover, occludin knockdown by shRNA suppressed, whereas occludin re-expression restored, the TER response to capsaicin. Mechanistically, TRPV1 activation increased ERK1/2 and MLC2 phosphorylation. PD98059, an ERK1/2 kinase inhibitor, abolished the capsaicin-induced MLC2 phosphorylation, whereas ML-7, an MLC2 kinase inhibitor, did not affect ERK1/2 phosphorylation, suggesting that ERK1/2 is the upstream signaling molecule of MLC2. Capsaicin also induced F-actin reorganization, which was abolished by CPZ, PD98059 and ML-7, indicating that TRPV1 activation altered F-actin organization in an ERK1/2- and MLC2-dependent manner. Furthermore, either PD98059 or ML-7 could abolish the capsaicin-induced TER response and occludin redistribution, whereas knockdown of ERK1/2 further confirmed that the TRPV1-modulated paracellular permeability was ERK1/2 dependent. Taken together, these results identified a crucial role of occludin in submandibular epithelial cells, and more importantly, demonstrated that occludin was required to mediate TRPV1-modulated paracellular permeability.

Key words: Occludin, Submandibular gland, Tight junction, Transient receptor potential vanilloid subtype 1

Introduction

Tight junctions are cell–cell interactions that form a primary barrier to the diffusion of materials through the paracellular route. As a complex, tight junctions are composed of transmembrane proteins, such as occludin and claudin family members, together with intracellular scaffold proteins such as zonula occludens-1 (ZO-1) (Tsukita et al., 2001). Occludin was the first identified transmembrane protein of tight junctions, and it has received much attention since its molecular characterization (Furuse et al., 1993; Balda et al., 1996; McCarthy et al., 1996; Balda et al., 2000). Occludin is found to be expressed in almost all epithelial tight junction structures, acting as an invariant component. Although subsequent studies showed that occludin may not be necessary in the formation of tight junctions, it is still indispensable in the regulation of paracellular barrier function (Saitou et al., 1998; Saitou et al., 2000).

Saliva secretion across the salivary epithelium can be accomplished by either the transcellular or paracellular route (Kawedia et al., 2007). It has been reported that, in addition to the

aquaporin-5-mediated transcellular transport, the salivation induced by agonists such as carbachol and isoproterenol also involves increased paracellular permeability (Segawa, 1994; Murakami et al., 2001; Hashimoto and Murakami, 2009). To date, occludin has been found in human, rat and mouse major salivary glands (Peppi and Ghabriel, 2004; Kawedia et al., 2007; Lourenço et al., 2007). In murine submandibular gland (SMG) carcinoma cells, the expression of an N-terminally truncated occludin construct causes a decrease in transepithelial electrical resistance (TER) as well as an increase in paracellular permeability (Bamforth et al., 1999). The expression and distribution of occludin, as well as other tight junction components are altered in the labial salivary gland of Sjögren's syndrome patients, suggesting that occludin can be a target for pathological factors and therefore be involved in the pathogenesis of salivary dysfunction (Ewert et al., 2010). However, the exact role of occludin in regulation of saliva secretion remains unclear.

Transient receptor potential vanilloid subtype 1 (TRPV1) is a ligand-gated nonselective cation channel that can be activated by

heat, low pH, and by capsaicin, the main pungent ingredient in chilli peppers (Caterina et al., 1997). TRPV1 was originally found to be expressed in neural cells. However, it has been shown that a functional TRPV1 is expressed in various tissues and cells, including bladder and bronchial epithelial cells, keratinocytes and pancreatic islet β cells (Veronesi et al., 1999; Birder et al., 2001; Inoue et al., 2002; Akiba et al., 2004). Activation of the peripheral TRPV1 mediates Ca^{2+} entry and increases cytosolic Ca^{2+} concentration, thereby eliciting diverse physiological functions other than nociceptive transduction. We previously demonstrated that TRPV1 is expressed in both human and rabbit SMG cells, and TRPV1 activation by capsaicin induces saliva secretion (Zhang et al., 2006; Ding et al., 2010). We also found that capsaicin increases paracellular permeability of rabbit SMGs (Cong et al., 2012), suggesting that the salivation induced by capsaicin is, at least in part, by increasing paracellular transport. However, the involvement of occludin in TRPV1-modulated paracellular permeability was still undetermined.

Therefore, the present study was designed to explore the potential role of occludin in modulating paracellular permeability and relevant signaling pathways in salivary epithelium using SMG-C6 cells. Our results showed that both TRPV1 and occludin were expressed in SMG-C6 cells. Activation of TRPV1 induced redistribution of occludin, paralleling the increased paracellular permeability. These effects were accomplished through ERK1/2 and its underlying MLC2/F-actin signaling pathway. Furthermore, knockdown of occludin not only decreased TER values of SMG-C6 cells at basal levels, but also abolished TRPV1-induced decrease in TER values. Together, these results suggested a crucial role of occludin in the submandibular tight junction barrier. More importantly, occludin was required to mediate TRPV1-modulated paracellular transport, perhaps by the capsaicin-activated ERK1/2/MLC2 signaling pathway.

Results

TRPV1 and occludin are expressed in SMG-C6 cells

Expression of TRPV1 mRNA was detected at the expected size of 258 bp in SMG-C6 cells (Fig. 1A), and further confirmed by sequencing. Rat dorsal root ganglion (DRG), reported to express TRPV1, was used as positive control. TRPV1 protein was observed with a molecular mass of ~ 95 kDa (Fig. 1A). Immunofluorescence imaging showed that TRPV1 proteins were widely diffused in the cytoplasm with a stronger intensity at the cell boundary (Fig. 1B). To further confirm the intracellular location of TRPV1, sequential images of the monolayer of cells at six different x - y planes from the apical surface to the basal region along the z -axis were taken using confocal microscopy. Consistently, TRPV1 protein was seen mainly in the cytoplasm and lateral membranes of SMG-C6 cells (Fig. 1C). We also co-stained cells with two lateral membrane markers, E-cadherin and β -catenin, which are components of adherens junctions. Images from both horizontal and vertical planes showed that TRPV1 was colocalized with E-cadherin and β -catenin (Fig. 1D). Moreover, 10 $\mu\text{mol/l}$ capsaicin treatment for 10 min did not induce any change in the distribution of TRPV1, E-cadherin or β -catenin (Fig. 1D). In accordance with the co-immunofluorescence results, immunoprecipitation assays identified that TRPV1 was co-precipitated with lateral membrane markers E-cadherin and β -catenin, but not with the apical tight junction component occludin (Fig. 1E). Additionally, the interaction between TRPV1 with either E-cadherin or β -catenin was not influenced by capsaicin

(Fig. 1E), which indicated that neither TRPV1 nor adherens junction distribution was altered after capsaicin treatment.

Previous data showed that a series of tight junction proteins including zonula occludens-1 (ZO-1), occludin, claudin-1, -3, -4 and -5 exist in rat SMG tissue (Peppi and Ghabriel, 2004). Thus, we examined these components in SMG-C6 cells and found that ZO-1, occludin, claudin-1, -3 and -4 mRNA were expressed, whereas claudin-2 and -5 mRNA were not detected (supplementary material Fig. S1A). Occludin mRNA at the expected size of 482 bp, and the protein (65 kDa) were detected in SMG-C6 cells (Fig. 1F). Occludin protein was continuously expressed in the cell membrane encircling the cells and delineating the cellular borders. Vertical x - z plane images further revealed that occludin was located in the most apical portion of cell membrane, whereas TRPV1 was expressed in the cytoplasm around the nucleus as well as the lateral membrane beneath occludin (Fig. 1G).

Activation of TRPV1 induces redistribution of occludin

Previous studies showed that proper distribution of occludin in the cell membrane is required for its normal performance, and occludin internalization is closely associated with barrier disruption (Musch et al., 2006; Marchiando et al., 2010; Van Itallie et al., 2010). After stimulation for 5 min with 10 $\mu\text{mol/l}$ capsaicin, occludin staining appeared to be reduced and more fragmented in the cell-cell contacts, while more positive staining increased in cytoplasm, which indicated that occludin was redistributed from the membrane into the cytoplasm. The redistributed occludin was partly returned to the membrane after capsaicin treatment for 60 min (Fig. 2A, upper panels). By contrast, the distribution of claudin-3, another transmembrane tight junction component expressed in SMG-C6 cells, was not affected by capsaicin (Fig. 2A, lower panels). Moreover, we extracted the cytoplasm and membrane protein fractions as previously described (Kawedia et al., 2008). Capsaicin induced a significant increase in occludin protein in the cytoplasm fraction within 60 min, together with a decrease in the membrane fraction. However, the claudin-3 content of both the cytoplasm or membrane fractions did not show any changes (Fig. 2B). These results were consistent with the immunofluorescence images, which demonstrated that capsaicin selectively induced redistribution of occludin, but not claudin-3.

The double immunofluorescence staining of occludin and claudin-3 from both horizontal (x - y) and vertical (x - z) planes revealed that occludin and claudin-3 were co-localized in SMG-C6 cells (Fig. 3A, upper panel). After exposure to 10 $\mu\text{mol/l}$ capsaicin for 10 min, occludin was disrupted and redistributed whereas claudin-3 was unaffected. In x - z images occludin appeared to become more dispersed and was no longer co-localized with claudin-3 (Fig. 3A, middle panel). The distribution of claudin-4, which forms a chloride-selective channel in other types of epithelia (Hou et al., 2010), was also observed by double-staining with occludin. Similar to claudin-3, there was no change in claudin-4 distribution after capsaicin treatment (10 $\mu\text{mol/l}$ for 10 min; Fig. 3A, lower panel), suggesting that both claudin-3 and claudin-4 might serve as invariant components in the tight junction complex, whereas occludin could be redistributed by capsaicin.

Previous studies reported that other cell-cell interaction components such as the adherens junction protein E-cadherin may also affect tight junction formation and regulate barrier

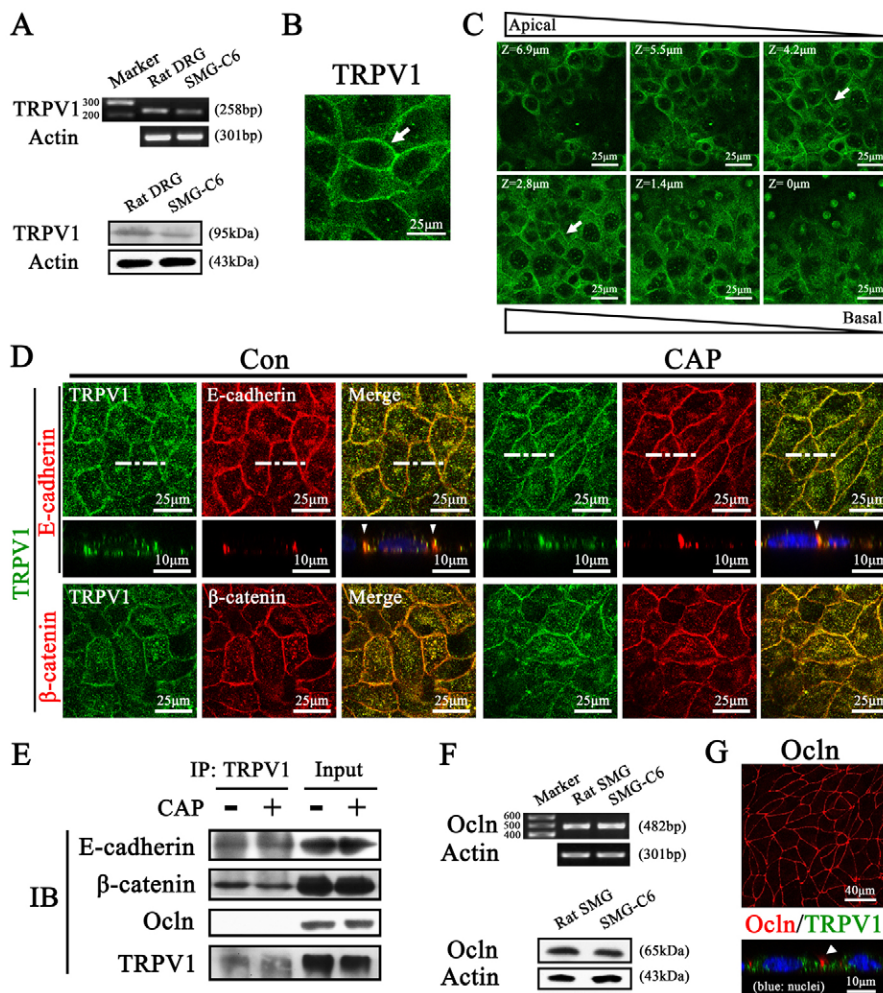


Fig. 1. TRPV1 and occludin are expressed in rat SMG-C6 cells. (A) Upper panels: RT-PCR analysis of TRPV1 mRNA in SMG-C6 cells. Rat dorsal root ganglion (DRG) was used as the positive control, and actin as the loading control. Lower panels: western blot analysis of TRPV1 expression in rat DRG and SMG-C6 cells. Equal loading of each lane was verified by actin. (B) Immunofluorescence staining of TRPV1 in SMG-C6 cells. TRPV1 protein was expressed in the cytoplasm of SMG-C6 cells with a stronger staining in the cell borders (white arrows). (C) Sequential images of SMG-C6 cells at six x-y planes along the z-axis showing that the TRPV1 was mainly in the lateral membranes (white arrows). Each image is a representative of three separate experiments in duplicate. Scale bars: 25 µm. (D) Co-immunofluorescence staining of TRPV1 with E-cadherin (upper and middle panels) or β-catenin (lower panel) with or without 10 µmol/l capsaicin treatment for 10 min. White lines in the x-y panels indicate the position of the z-line scans; white arrowheads point to the co-localization of TRPV1 and E-cadherin in the x-z images. Each image is a representative of three separate experiments in duplicate. Scale bars for the x-y and x-z images: 25 µm and 10 µm, respectively. (E) Co-immunoprecipitation of TRPV1 with E-cadherin, β-catenin or occludin (Ocld). TRPV1 co-precipitated with either E-cadherin or β-catenin, and their interactions did not change after capsaicin treatment. In contrast, TRPV1 did not co-precipitate with occludin. (F) Upper panels: RT-PCR analysis of occludin mRNA in SMG-C6 cells. Rat submandibular gland (SMG) tissue was used as a positive control. Lower panels: western blot analysis of occludin expression in rat SMG tissue and SMG-C6 cells. (G) Immunofluorescence staining of occludin. X-y images show that occludin protein is located in the cell membrane of SMG-C6 cells. Scale bars: 10 µm and 40 µm. X-z images show that occludin is located in the most apical portion of cell membrane (white arrowheads), while TRPV1 is expressed in the cytoplasm as well as the lateral membrane beneath occludin. Scale bars: 10 µm. Each image is a representative of three separate experiments in duplicate.

function (Tunggal et al., 2005). We thus investigated the effect of capsaicin on the distribution of occludin and E-cadherin simultaneously. Under unstimulated conditions, both occludin and E-cadherin were localized at the cell-cell contacts; however, x-z images clearly showed that E-cadherin was positioned directly below occludin (Fig. 3B). As capsaicin (10 µmol/l for 10 min) induced a redistribution of occludin as described above, the location of E-cadherin was unaffected in either x-y or x-z images (Fig. 3B). These results indicated that capsaicin selectively induced occludin redistribution, but not E-cadherin. Furthermore, pre-incubation for 30 min with 10 µmol/l capsazepine (CPZ), a TRPV1 antagonist, abolished the capsaicin-induced redistribution

of occludin, whereas CPZ alone did not alter the membrane distribution of occludin (Fig. 3B). DMSO was used as the vehicle control (data not shown). We further quantified the proportion of cells in which occludin had been redistributed in lower magnification images of at least 100 cells. Capsaicin (10 µmol/l for 10 min) induced breaks in staining greater than 4 µm in $42.3 \pm 6.81\%$ of cells, a significant increase compared with $4.8 \pm 2.08\%$ in unstimulated cells, $5.4 \pm 1.73\%$ in CPZ+CAP-treated cells, and $4.7 \pm 2.31\%$ in CPZ-treated cells. Together these data suggested that capsaicin selectively induced the redistribution of occludin, but not claudin-3 or E-cadherin, in SMG-C6 cells through activation of TRPV1.

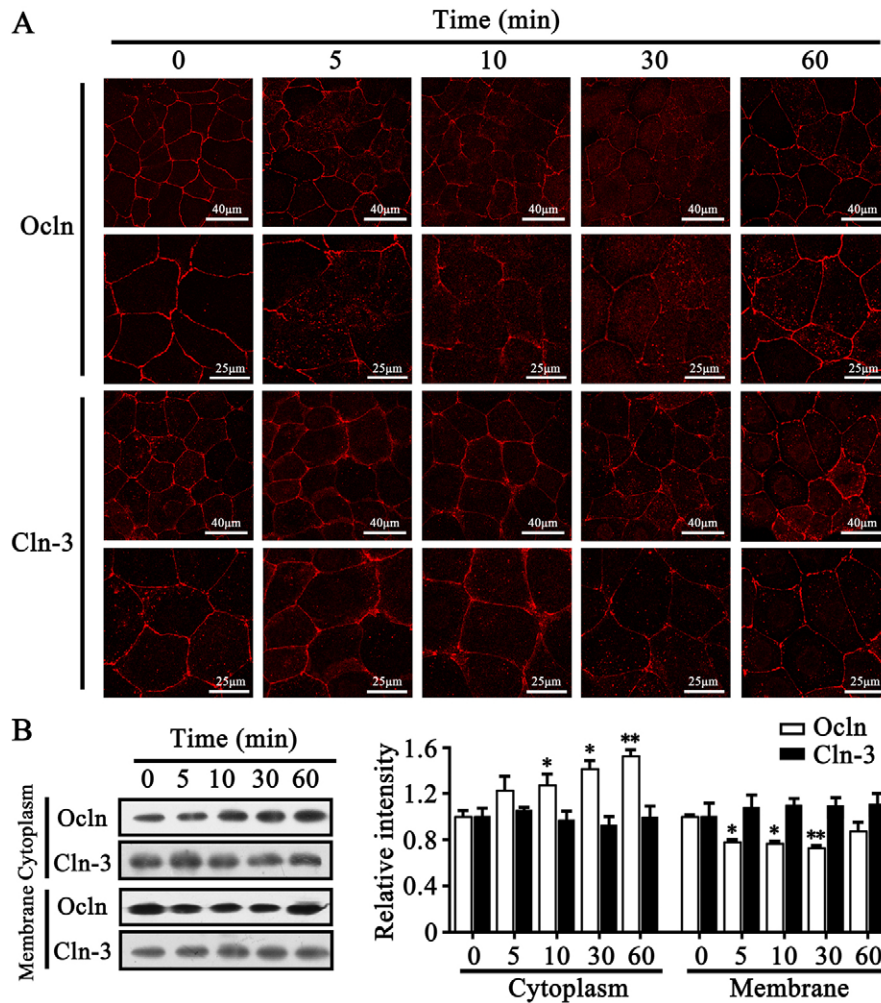


Fig. 2. Capsaicin induces redistribution of occludin. (A) Immunofluorescence imaging of occludin (Ocln) and claudin-3 (Cln-3) distribution induced by capsaicin. A reduction and discontinuity of occludin was observed in the cell membrane, along with more intracellular staining after 10 $\mu\text{mol/l}$ capsaicin treatment for 5, 10 and 30 min, but by 60 min the membrane localization of occludin was partly recovered. However, the distribution of claudin-3 was not influenced by capsaicin treatment. Images of both occludin and claudin-3 are shown at two magnifications (scale bars: 40 μm and 25 μm). Each image is representative of three separate experiments in duplicate. (B) Capsaicin-induced expression of occludin and claudin-3 in the cytoplasmic and membrane fractions. Left: capsaicin (10 $\mu\text{mol/l}$) significantly increased occludin protein expression in the cytoplasmic fraction within 60 min, but reduced its expression in the membrane fraction. In contrast, the expression of claudin-3 in these two fractions was unaffected by capsaicin. Right: quantitative analysis of occludin and claudin-3 in cytoplasmic and membrane fractions. * $P < 0.05$ and ** $P < 0.01$ compared with unstimulated cells.

Activation of TRPV1 decreases TER and increases paracellular transport

To further evaluate the effect of TRPV1 activation on tight junction function, TER and paracellular permeability assays were performed as described previously (Turner et al., 1997; Sáenz-Morales et al., 2009). In SMG-C6 cells, the initial TER value was $516.2 \pm 98.62 \Omega\text{-cm}^2$, which was consistent with previous reports in the same cell line (Kawedia et al., 2008) and represented a relatively 'tight' epithelium according to the description of electrical characteristics (Anderson and Van Itallie, 2009). 1 $\mu\text{mol/l}$ capsaicin did not induce any change to TER values within 60 min (Fig. 4A), whereas at 5 $\mu\text{mol/l}$, only a small but significant decline in TER value appeared at 60 min (Fig. 4B). At 10 and 20 $\mu\text{mol/l}$, capsaicin evoked a rapid and prominent drop in TER values from 5 to 60 min (Fig. 4C,D). Pretreatment with 10 $\mu\text{mol/l}$ CPZ for 30 min abolished the 10 $\mu\text{mol/l}$ capsaicin-induced TER decrease, while DMSO alone did not affect TER values (Fig. 4E). Serving as a positive control, incubation of SMG-C6 cells in a Ca^{2+} -free medium for 60 min caused a dramatic twofold decrease in TER values (Fig. 4E) due to its effects on tight junction disassembly and paracellular opening as previously reported.

It is well known that TRPV1 influences diverse activities through Ca^{2+} signaling. Here, we showed that 10 $\mu\text{mol/l}$ capsaicin increased the mean and median Fluo-3 fluorescence

in the 30,000 harvested cells at 60 s by flow cytometry (Burchiel et al., 2000), which indicated that capsaicin evoked an initial small peak of intracellular Ca^{2+} ($[\text{Ca}^{2+}]_i$). The $[\text{Ca}^{2+}]_i$ returned to basal level after capsaicin treatment for 300 s. Pretreatment with 10 $\mu\text{mol/l}$ CPZ for 30 min abolished the capsaicin-induced increased $[\text{Ca}^{2+}]_i$, whereas CPZ alone did not affect $[\text{Ca}^{2+}]_i$ (supplementary material Fig. S1B).

In addition to TER measurements, the paracellular permeability is also routinely evaluated by non-charged tracers, which can pass through the monolayer only by the paracellular route. We used Trypan Blue and FITC-dextran as indicators, and calculated their flow rate as described previously (Sáenz-Morales et al., 2009; Rosenthal et al., 2010). Capsaicin significantly elicited a brief and transient approximately twofold increase in Trypan Blue flux during a 5–10 min period (Fig. 4F). The apparent permeability coefficients (P_{app}) for 4 kDa FITC-dextran were also greatly enhanced by capsaicin (Fig. 4G). These flux studies provided more evidence that capsaicin increased paracellular permeability of SMG-C6 cells.

Depletion or re-expression of occludin alters the response of capsaicin-induced TER

To reveal the potential role of occludin in paracellular permeability of SMG-C6 cells, we designed specific shRNAs to knock down the expression of occludin and claudin-3

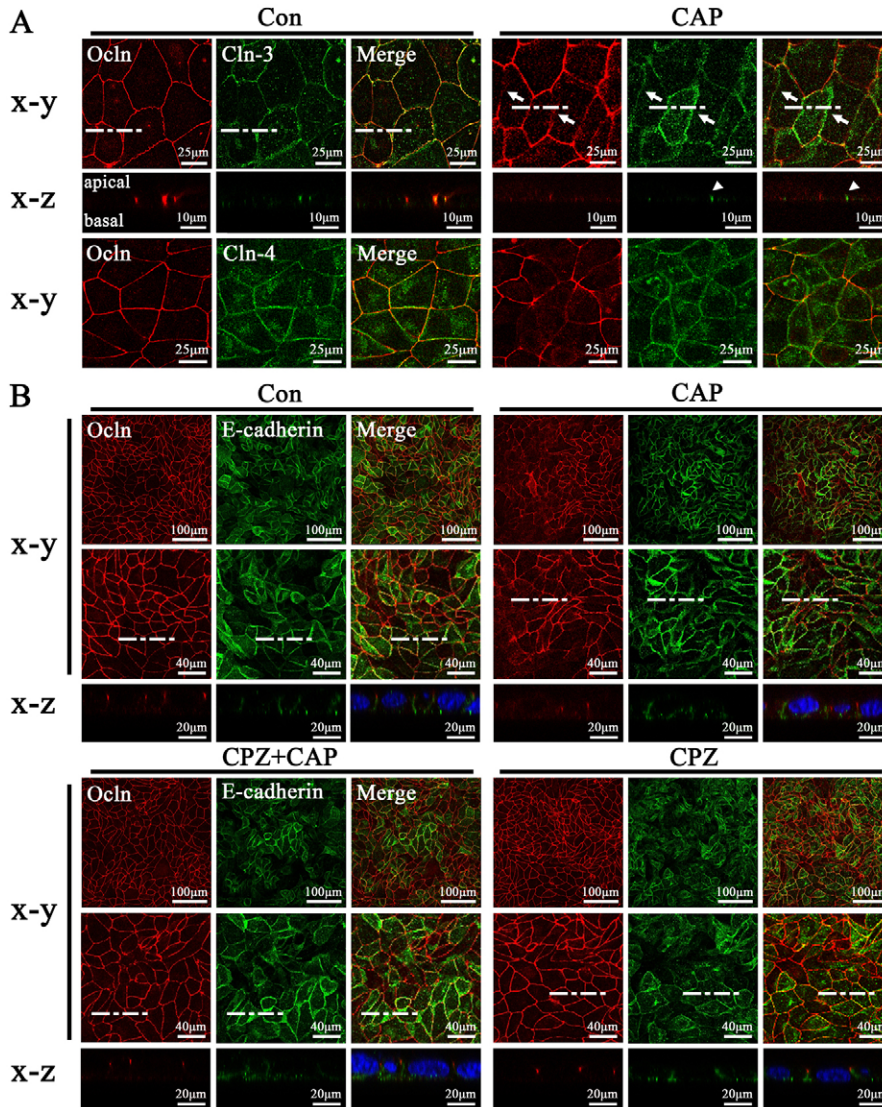


Fig. 3. Capsaicin induces occludin redistribution via activation of TRPV1. (A) Upper and middle panels: co-immunofluorescence imaging of occludin (Ocln) and claudin-3 (Cln-3). Lower panel: co-immunofluorescence imaging of occludin and claudin-4 (Cln-4). Occludin was co-localized with either claudin-3 or claudin-4 in unstimulated cells. Capsaicin ($10 \mu\text{mol/l}$ for 10 min) disrupted the occludin expression in the cell membrane (white arrows), whereas neither claudin-3 nor claudin-4 distribution was altered. X-z images show that occludin appeared more dispersed and was not co-localized with claudin-3 (white arrowheads). Each image is a representative of three separate experiments in duplicate. Scale bars for x-y and x-z images: $25 \mu\text{m}$ and $10 \mu\text{m}$, respectively. (B) Co-immunofluorescence imaging of occludin (Ocln) and E-cadherin after capsaicin treatment with or without capsazepine (CPZ) pretreatment. Both occludin and E-cadherin localized at the cell-cell contacts in x-y images, and E-cadherin was positioned below occludin in x-z images. $10 \mu\text{mol/l}$ capsaicin caused an obvious internalization of occludin, but not E-cadherin. CPZ ($10 \mu\text{mol/l}$ for 30 min) abolished the capsaicin-induced occludin redistribution. Each image is representative of three separate experiments in duplicate. X-y images are shown at two magnifications (scale bars: $100 \mu\text{m}$ and $40 \mu\text{m}$); x-z images (scale bars: $20 \mu\text{m}$).

(Fig. 5A). Depletion of occludin significantly reduced the baseline TER value by 45.5% compared with scrambled control ($P < 0.01$), whereas depletion of claudin-3 slightly decreased the basal TER value by 20.3% but was not statistically significant (Fig. 5B). We then evaluated the involvement of those occludin or claudin-3 knockdown cells, in the TRPV1-modulated paracellular permeability. Compared with the scrambled control cells, knockdown of occludin significantly reduced TER responses to treatment with $10 \mu\text{mol/l}$ capsaicin from 5–60 min (Fig. 5C). By contrast, in claudin-3 knockdown cells, capsaicin still caused a prompt decline in TER values (Fig. 5D).

To further confirm that the disappearance of the TER response to capsaicin was due to occludin depletion but not other influencing factors, we re-expressed occludin ('rescue') by transfecting occludin cDNA into occludin knockdown cells. Compared with control scrambled siRNA-treated cells, the protein expression of occludin was recovered to 68.2% and TER value was restored to 80.9% in occludin rescue cells (Fig. 5E,F). Furthermore, the capsaicin-induced TER decrease re-appeared in occludin rescue cells (Fig. 5G). Together these results suggested that occludin, rather than claudin-3, plays a

crucial role in barrier function of SMG-C6 cells, and capsaicin-induced increases in paracellular permeability are predominantly mediated through occludin.

Activation of TRPV1 increases ERK1/2 phosphorylation

We next explored the possible intracellular signaling pathway involved in the capsaicin-induced alteration of TER and occludin distribution. Extracellular signal-regulated kinase 1/2 (ERK1/2), p38 mitogen-activated protein kinase (p38MAPK), and c-Jun N-terminal kinase (JNK) are major members of the MAPK family and have been suggested to play important roles in mediating tight-junction protein expression and function in different tissues and cells (González-Mariscal et al., 2008). We found that the p-ERK1/2 level was significantly increased at 5 and 10 min, and returned to the basal level at 30 min after $10 \mu\text{mol/l}$ capsaicin treatment (Fig. 6A). However, the levels of p-p38MAPK and p-JNK were not changed at these times (supplementary material Fig. S1C). The total amounts of ERK1/2, p38MAPK and JNK did not change by capsaicin treatment. The results suggested that ERK1/2, but not p38MAPK or JNK, was the downstream signaling molecule selectively regulated by capsaicin.

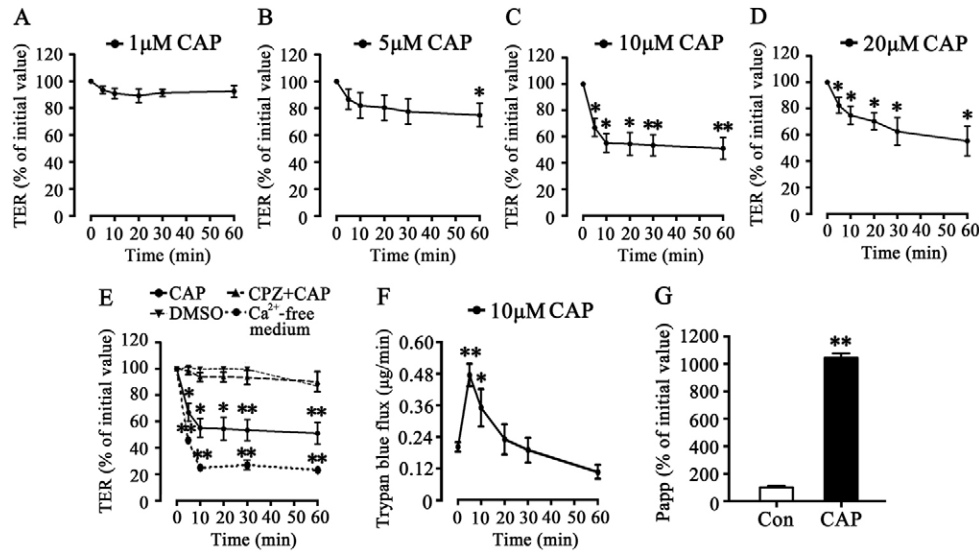


Fig. 4. Activation of TRPV1 increases paracellular permeability of SMG-C6 cells. Time course of TER was measured using an EVOM. (A) 1 μmol/l capsaicin (CAP) had no effect on TER values within 60 min. (B) 5 μmol/l capsaicin caused a small but significant decrease at 60 min. (C) 10 μmol/l or (D) 20 μmol/l capsaicin evoked a rapid decrease in TER from 5 to 60 min. (E) Capsazepine (CPZ, 10 μmol/l for 30 min) suppressed capsaicin-induced TER decrease. Incubation of cells in a Ca²⁺-free medium caused a decrease in TER values from 5 to 60 min. (F) Time course of Trypan Blue transport into the lower chamber medium. The flux of Trypan Blue was transiently increased after capsaicin treatment for 5–10 min. (G) The apparent permeability coefficients (P_{app}) for 4 kDa FITC-dextran was also increased by capsaicin (10 μmol/l for 10 min). Values are means \pm s.d. from three independent experiments performed in duplicate. * P <0.05 and ** P <0.01 compared with unstimulated cells.

Pretreatment with CPZ (10 μmol/l for 30 min) abolished capsaicin-induced ERK1/2 phosphorylation (Fig. 6B), further indicating that capsaicin induced ERK1/2 activation through TRPV1.

Capsaicin increases MLC2 phosphorylation in an ERK1/2-dependent manner

Myosin light chain 2 (MLC2) is a member of the regulatory light chain of myosin II, and plays a crucial role in regulating the distribution of tight junctions as well as the paracellular permeability in epithelial cells (Hecht et al., 1996; Shen et al., 2006). We explored the effect of capsaicin on MLC2 phosphorylation and the relationship between ERK1/2 and MLC2 in SMG-C6 cells. Phosphorylation of MLC2 at Ser19 was significantly elevated at 5 min, peaked at 10 min, and returned to basal level at 30 min after capsaicin treatment (Fig. 6C). Pre-incubation with ML-7 (20 μmol/l), an inhibitor of MLC2 upstream kinase, for 30 min did not affect the capsaicin-induced ERK1/2 phosphorylation. However, pretreatment with PD98059 (20 μmol/l), an inhibitor of ERK1/2 upstream kinase, for 30 min abolished the capsaicin-induced MLC2 phosphorylation (Fig. 6D). As shown in supplementary material Fig. S1D, the concentrations of PD98059 or ML-7 used in this study effectively inhibited their target kinases in SMG-C6 cells. These results indicated that MLC2 was downstream of ERK1/2 in SMG-C6 cells, and capsaicin activated MLC2 in an ERK1/2-dependent manner.

Activation of TRPV1 alters F-actin organization in an ERK1/2- and MLC2-dependent manner

Since F-actin has a direct structural link with the tight-junction complex, any influence on F-actin organization could alter tight junction distribution as well as paracellular permeability (Bruewer et al., 2004; Peixoto and Collares-Buzato, 2005).

Therefore, we examined the effect of capsaicin on F-actin organization. Under unstimulated condition, a high density of F-actin was present at the peri-junctional regions with abundant stress fibers in the cytoplasm of SMG-C6 cells. However, F-actin architecture was disorganized after capsaicin (10 μmol/l) treatment for 5, 10 and 30 min. A significant decrease in the stress fibers and more F-actin at the cell periphery, together with an obvious increased space between adjacent F-actin filaments was seen at those time points, whereas it was partly recovered after capsaicin treatment for 60 min (Fig. 6E). CPZ pretreatment (10 μmol/l for 30 min) abolished capsaicin-induced F-actin reorganization (Fig. 6E). Co-staining of F-actin and E-cadherin further showed that capsaicin reorganized F-actin in particular while the distribution of E-cadherin was unaffected (Fig. 6F, upper panel). To further clarify whether this increased peripheral F-actin was at cell–cell junctions, co-staining of F-actin with occludin was performed. Results showed that the displacement of occludin occurred with an increased F-actin staining close to the occludin position, indicating that F-actin was assembled near the cell–junction region by capsaicin treatment (Fig. 6F, lower panel).

We also identified the effects of ERK1/2 and MLC2 on F-actin organization. Pretreatment with either PD98059 or ML-7 for 30 min abolished the capsaicin-induced F-actin reorganization, whereas PD98059 and ML-7 alone, as well as DMSO, had no effect on F-actin morphology (Fig. 6G, upper panel). Co-immunofluorescence images of F-actin and E-cadherin showed that the disrupted stress fiber organization, as well as the junctional reorganization of F-actin was restored by PD98059 and ML-7 pretreatment (Fig. 6G, lower panel). These results suggested that both ERK1/2 and MLC2 were required in TRPV1-modulated F-actin organization. Cytochalasin B (CytoB) or Ca²⁺-free medium were used as the positive control (Bengtsson et al., 1993; Nybom and Magnusson, 1996; Schaphorst et al., 2003).

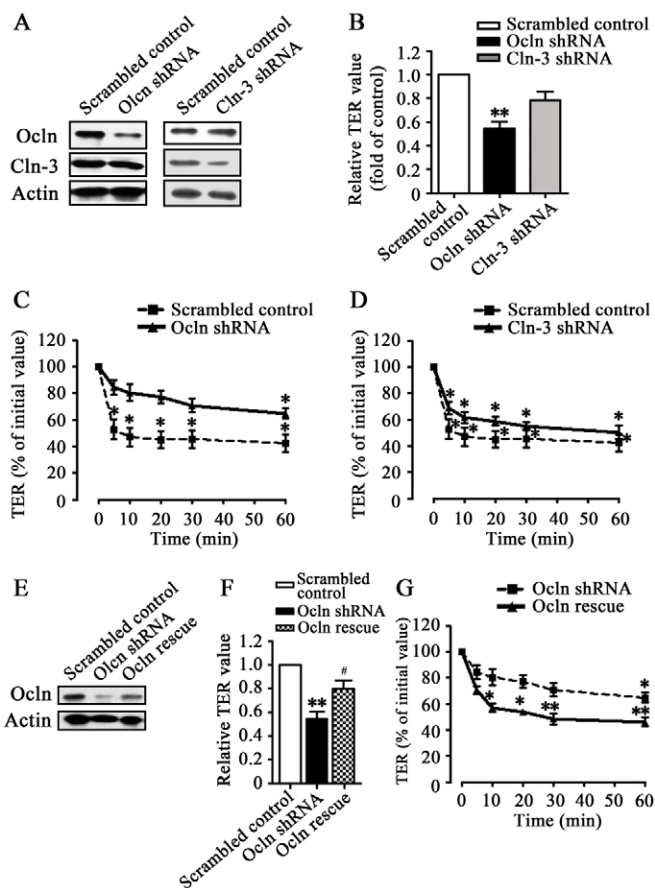


Fig. 5. Occludin is required to mediate capsaicin-induced increased paracellular permeability. (A) Western blot of occludin (Ocln) and claudin-3 (Cln-3) in SMG-C6 cells that were transfected with occludin and claudin-3 shRNAs, respectively. Occludin shRNA induced a decrease in occludin protein levels, but no change in claudin-3 expression. Claudin-3 shRNA induced a decrease in claudin-3 protein levels, but no change in occludin expression. (B) Knockdown of occludin significantly reduced TER value compared with control, whereas knockdown of claudin-3 only slightly decreased TER value. (C) The capsaicin-induced decreases in TER were inhibited in occludin knockdown cells. (D) Claudin-3 knockdown did not affect the capsaicin-reduced TER values. (E) Western blot of occludin in the 'rescue' cells by transfection of occludin cDNA into the occludin knockdown cells. The expression of occludin in the rescue cells was upregulated compared with that in occludin knockdown cells. (F) TER value in the rescue cells was also restored. (G) The capsaicin-induced decline in TER was much less in occludin rescue cells. Values are means \pm s.d. from three independent experiments performed in duplicate. * P <0.05 and ** P <0.01 compared with unstimulated control. # P <0.05 compared with occludin knockdown cells.

CytoB (20 μ mol/l for 30 min) induced a disruption of actin filaments, and incubation of SMG-C6 cells in a Ca^{2+} -free medium for 60 min caused an obvious shrinkage of the filaments (Fig. 6G).

ERK1/2/MLC2 signaling pathway is involved in TRPV1-mediated paracellular permeability and occludin redistribution

The involvement of the ERK1/2 and MLC2 pathway in capsaicin-induced paracellular permeability and occludin distribution was further investigated. Pretreatment with either PD98059 or ML-7 for 30 min abolished the capsaicin-induced

decreases in TER (Fig. 7A,B), and meanwhile, suppressed capsaicin-induced redistribution of occludin (Fig. 7C), whereas PD98059 and ML-7 alone did not affect TER or occludin location. In addition, to demonstrate the crucial involvement of the cytoskeleton in capsaicin-induced occludin redistribution, we pretreated cells with either CytoB for 30 min or Ca^{2+} -free medium for 60 min and found that occludin expression in the cell membrane was dramatically disrupted and simultaneously the staining in the cytoplasm was increased (Fig. 7C). This suggested a crucial requirement of cytoskeleton organization for TRPV1-mediated occludin distribution. Quantification of the intensity of the occludin fluorescence in the cytosol showed that increased occludin in cytosol induced by capsaicin was significantly inhibited by either PD98059 or ML-7 pretreatment (Fig. 7D). Moreover, the increased expression of occludin in the cytoplasm and the decreased expression of occludin in membrane, was blocked by pretreatment with PD98059 and ML-7 for 30 min, respectively (Fig. 7E). These results again indicated that ERK1/2 and MLC2 signaling molecules are responsible for capsaicin-induced increased paracellular permeability and occludin redistribution.

We also treated SMG-C6 cells with scrambled control or ERK1/2-specific siRNA. The expression of total ERK1/2 was markedly reduced and capsaicin-induced increased p-ERK1/2 and p-MLC2 disappeared (Fig. 8A). More importantly, the decreases in both TER (Fig. 8B) and occludin redistribution induced by capsaicin were significantly attenuated by ERK1/2 knockdown (Fig. 8C), in parallel with the above results using ERK1/2 inhibitor, which again confirmed the importance of ERK1/2 in TRPV1-modulated paracellular permeability and occludin distribution.

Discussion

There are three major new findings presented by our study. First, we demonstrated that activation of TRPV1 increased paracellular permeability and altered occludin distribution in SMG-C6 cells. Second, by knockdown and re-expression, we revealed that occludin was a required component of tight junction barrier in SMG and played an important role in the capsaicin-induced increase in paracellular permeability. Third, ERK1/2 and the downstream signaling molecule MLC2 were responsible for the capsaicin-induced increase in paracellular permeability and occludin redistribution. These results provided new insights into the crucial role of occludin in forming a tight-junction barrier, and characterized a novel mechanism of TRPV1-modulated paracellular permeability in submandibular epithelium.

TRPV1 was originally found in the neural system, but more attention was recently focused on its non-neural expression and function (Inoue et al., 2002; Akiba et al., 2004; Saunders et al., 2007). We previously demonstrated that a functional TRPV1 is expressed in human and rabbit SMGs, and capsaicin-induced salivation partially involves an increased paracellular transport in rabbit SMGs (Zhang et al., 2006; Ding et al., 2010; Cong et al., 2012). However, the precise mechanism involved in TRPV1-modulated tight-junction barrier was still unknown. Because there is no appropriate cell line derived from either human or rabbit SMGs for further study on tight-junction structure and function, we chose the rat SMG-C6 cells to characterize the effect of TRPV1 on SMG epithelia. This cell line, originally established by Quissel et al., was reported to maintain a normal

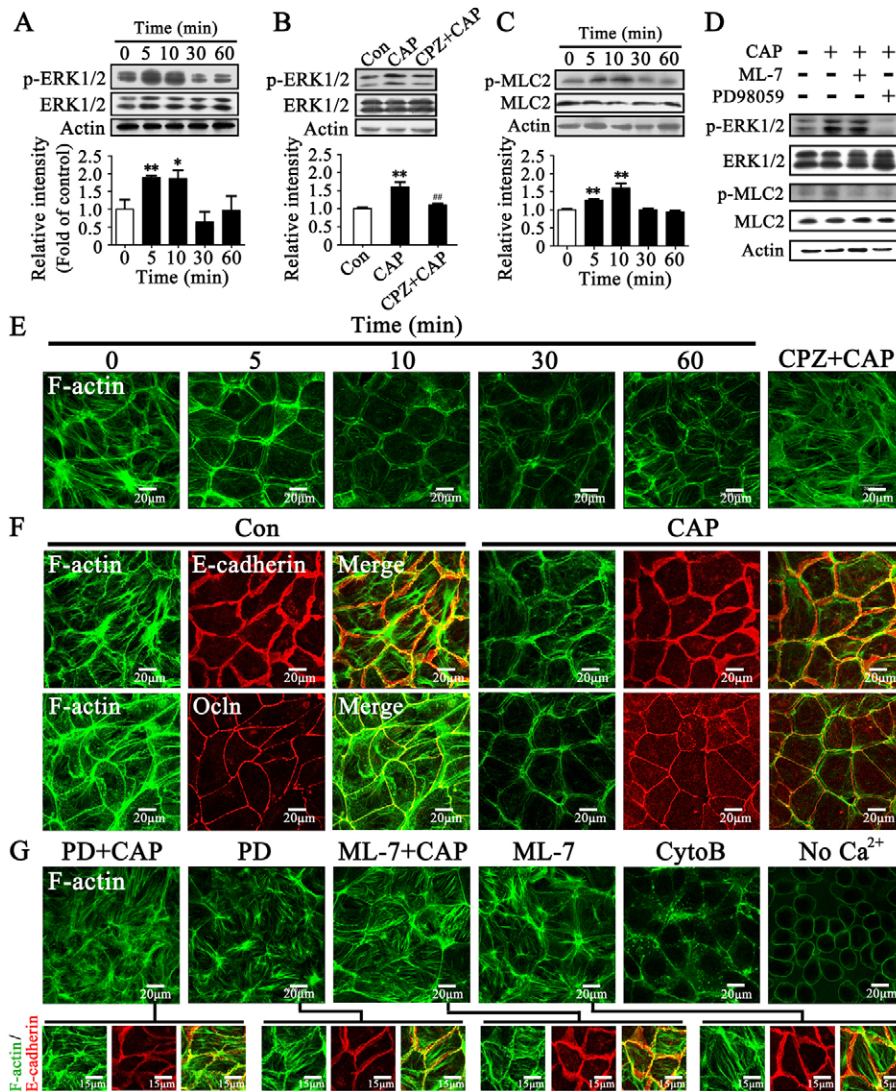


Fig. 6. Activation of TRPV1 increases ERK1/2 and MLC2 phosphorylation, and alters F-actin distribution. (A) The levels of p-ERK1/2 were significantly increased after 10 $\mu\text{mol/l}$ capsaicin treatment, while the total ERK1/2 level showed no change. (B) The capsaicin (CAP)-induced increase in p-ERK1/2 expression was suppressed by pretreatment with 10 $\mu\text{mol/l}$ capsapine (CPZ) for 30 min. (C) Phosphorylation of MLC2 at Ser19 was elevated by capsaicin treatment. Expression of total MLC2 did not change. Values are means \pm s.d. from three independent experiments performed in duplicate. * P <0.05 and ** P <0.01 compared with control. $^{###}P$ <0.01 compared with capsaicin-treated cells. (D) Pre-incubation with ML-7 (20 $\mu\text{mol/l}$) for 30 min had no effect on the capsaicin-induced ERK1/2 phosphorylation, whereas pretreatment with PD98059 (20 $\mu\text{mol/l}$) for 30 min abolished the MLC2 phosphorylation induced by capsaicin. (E) Immunofluorescence imaging of F-actin after capsaicin treatment for 5–60 min. Under unstimulated conditions, F-actin was mainly present at the peri-junctional regions with abundant stress fibers in the cytoplasm. However, the architecture of F-actin was disorganized, and a significant decrease in the stress fibers was observed after 10 $\mu\text{mol/l}$ capsaicin treatment. Moreover, the capsaicin-induced F-actin disorganization was inhibited by pretreatment with CPZ. (F) Co-immunofluorescence imaging of F-actin with either E-cadherin or occludin. Upper panel: capsaicin (10 $\mu\text{mol/l}$ for 10 min) reorganized F-actin, but the distribution of E-cadherin was not affected. Lower panel: capsaicin treatment resulted in the redistribution of both F-actin and occludin. (G) Both F-actin staining (upper panel) and F-actin/E-cadherin co-staining (lower panel) showed that pretreatment with either PD98059 or ML-7 abolished the capsaicin-induced F-actin redistribution, while PD98059 and ML-7 alone had no effect on F-actin organization. Incubation with cytochalasin B (CytoB, 20 $\mu\text{mol/l}$ for 30 min) or Ca^{2+} -free medium were used as positive controls. Each image is a representative of three separate experiments in duplicate.

acinar function and have similar characteristics, including tight junction structure, as determined by electron microscopy (Quissell et al., 1997). In the present study, we confirmed the expression of TRPV1 and occludin and characterized their distribution. We also identified a similar expression pattern for several other proteins including ZO-1, occludin and claudin-1, -3 and -4 in SMG-C6 cells in rat SMG tissue to those previously reported, except for claudin-5, which was particularly localized

in endothelial cells of microvessels of SMG (Peppi and Ghabriel, 2004). The similarities suggested that SMG-C6 could be a suitable cell model to study the effect of TRPV1 activation on tight-junction barriers of submandibular epithelia.

Isoda et al. first reported that capsaicin increases paracellular permeability of intestinal Caco-2 cells via TRPV1 activation (Isoda et al., 2001). Reiter et al. showed that activation of TRPV4, another member of the transient receptor potential (TRP)

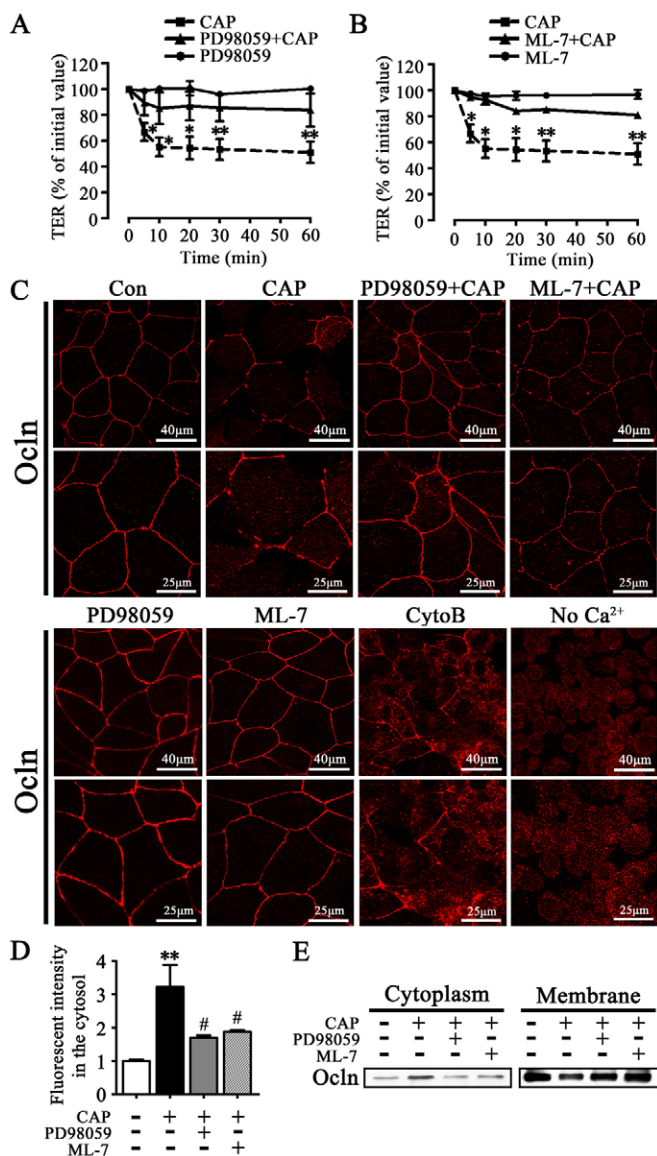


Fig. 7. ERK1/2 and MLC2 are involved in capsaicin-induced paracellular permeability and occludin redistribution. Pretreatment with either 20 $\mu\text{mol/l}$ PD98059 (A) or 20 $\mu\text{mol/l}$ ML-7 (B) for 30 min abolished the capsaicin (CAP)-induced decreases in TER values. Values are means \pm s.d. from three independent experiments performed in duplicate. * $P < 0.05$ and ** $P < 0.01$ compared with unstimulated cells. (C) Pretreatment with either PD98059 or ML-7 suppressed capsaicin-induced redistribution of occludin. Incubation with cytochalasin B (CytoB, 20 $\mu\text{mol/l}$ for 30 min) or Ca^{2+} -free medium for 60 min dramatically disrupted occludin distribution in the membrane. Each image is a representative of three separate experiments in duplicate. Scale bars for the lower and higher magnification images: 40 μm and 25 μm , respectively. (D) The quantitative analysis of the fluorescence intensity of occludin in the cytosol. The capsaicin-induced increase in cytosolic occludin was significantly inhibited by either PD98059 or ML-7 pretreatment. ** $P < 0.01$ compared with unstimulated cells. # $P < 0.05$ compared with capsaicin-treated cells. (E) Pretreatment with either PD98059 or ML-7 abolished the capsaicin-induced increase in occludin expression in the cytoplasm fraction, as well as the decreased occludin expression in the membrane fraction.

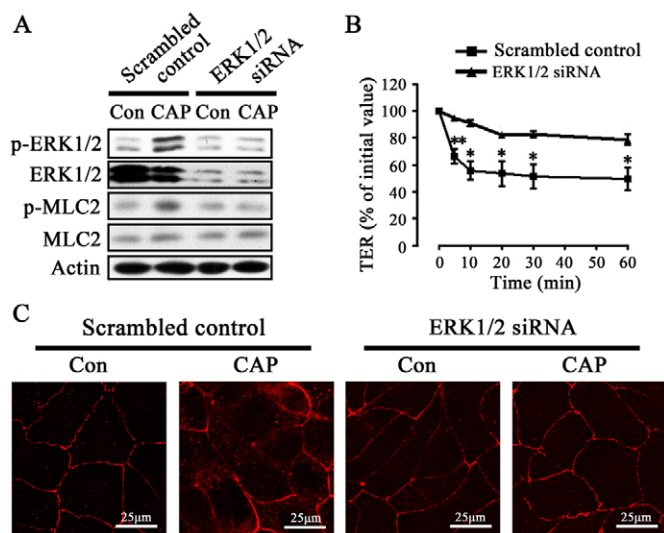


Fig. 8. The capsaicin-induced decrease in TER values and occludin redistribution does not occur in ERK1/2 knockdown cells. (A) Expression of ERK1/2 and MLC2 in SMG-C6 cells that were transfected with ERK1/2 siRNA. The expression of total ERK1/2 was markedly decreased and capsaicin-induced increases in p-ERK1/2 and p-MLC2 did not occur. (B) The capsaicin-induced decreases in TER were attenuated in ERK1/2 knockdown cells. Values are means \pm s.d. from three independent experiments performed in duplicate. * $P < 0.05$ and ** $P < 0.01$ compared with unstimulated cells. (C) The capsaicin-induced occludin redistribution did not occur in ERK1/2 knockdown cells. Each image is a representative of three separate experiments in duplicate. Scale bars: 25 μm .

superfamily, enhances epithelial paracellular permeability in the mammary cell line HC11 (Reiter et al., 2006). Here, we provided new evidence that activation of TRPV1 increased paracellular permeability in SMG-C6 cells, as characterized by a rapid decrease in TER and a significant increase in paracellular flux of Trypan Blue and FITC-dextran. In currently accepted models of saliva secretion, the active transcellular Cl^- accompanied with paracellular Na^+ transport is the primary driving force for fluid and electrolyte secretion by acinar cells. Since the apical Cl^- channel is Ca^{2+} -dependent, and activation of TRPV1 elevates $[\text{Ca}^{2+}]_i$, many studies have reported that TRPV1 activates Cl^- channels in various epithelial cells (Lee et al., 2005; Auzanneau et al., 2008). Therefore, whether TRPV1 activation could trigger an increase in Cl^- movement through the opening of Ca^{2+} -dependent Cl^- channels in salivary epithelium needs to be further investigated.

Overexpression of occludin in MDCK II monolayers increases TER as well as paracellular flux, implying its involvement in the function of the tight-junction barrier (Balda et al., 1996). Although occludin knockout mice had physiologically and structurally normal tight junctions, they still displayed numerous epithelial or endothelial abnormalities, such as chronic gastric inflammation and hyperplasia, calcification in the brain, testicular atrophy and dysfunction of the salivary gland (Saitou et al., 2000). Several studies have described that exposure of intestinal cells to cytokines, bacteria, toxins and viruses results in a disruption of tight-junction structure and leads to endocytosis of occludin, together with decreases in TER and increases in paracellular permeability (Yu and Turner, 2008; Coyne et al., 2007; Liu et al., 2009). Remarkably, a recent study showed that

overexpression of occludin enhances, and occludin knockdown declines, cytokine-induced increased TER and decreased permeability of large solutes (Van Itallie et al., 2010). Although the results seem not to be completely consistent with the previously report by Balda et al., they have still provided clear evidence that occludin plays an indispensable part in determining barrier function (Balda et al., 1996). However, up to now, limited data was available on the significance of occludin in salivary epithelium. In the rat parotid gland epithelial cell line Pa-4, occludin acts as a pivotal molecule in oncogenic Raf-1-induced disruption of tight-junction barriers (Li and Mrsny, 2000). Mutation of occludin disrupts tight-junction structure and barrier function in murine SMG carcinoma cells (Bamforth et al., 1999). Alteration of the expression and localization of occludin has been shown in the labial salivary glands from Sjögren's syndrome patients (Ewert et al., 2010). These studies indicated that occludin might play a crucial role in salivary epithelium. In the present study, we provided additional evidence that knockdown of occludin, but not claudin-3, resulted in a significant drop in TER, and occludin 'rescue' restored paracellular permeability in SMG-C6 cells, suggesting a critical requirement of occludin in forming the tight-junction barrier of submandibular cells. However, occludin knockdown only partially reversed the capsaicin-induced decrease in TER values, so there could be other synergistic or distinct factors that regulate paracellular permeability following TRPV1 activation. For example, the modulation of apical Ca^{2+} -dependent Cl^- as mentioned above, could also influence solute transport through the paracellular route. Thus, more evidence should be provided in the future to support our hypothesis.

The abnormal redistribution of occludin from the cell membrane into the cytoplasm triggered by various stimuli is a common feature of tight-junction injury and is closely associated with physiological barrier disruption (Shifflett et al., 2005; Van Itallie et al., 2010). Here, we showed that TRPV1 activation caused redistribution of occludin from the cell membrane, but did not affect the continuity of claudin-3, claudin-4, E-cadherin or β -catenin. Moreover, knockdown of occludin abolished, and re-expression of occludin recovered, capsaicin-induced decreased TER. These data demonstrated occludin, rather than claudin-3, claudin-4, E-cadherin and β -catenin, plays a crucial role in capsaicin-modulated the tight-junction barrier in SMG-C6 cells.

In the previous study, we found that activation of TRPV1 upregulates expression of ZO-1, claudin-3 and -11 in rabbit SMG tissues (Cong et al., 2012). However, in the present study, the distribution of claudin-3 in rat SMG cells was unaffected by capsaicin. An explanation for the discrepant results might be the different tight-junction expression patterns of the two species. Another possible reason is that the present work showed only a short-term effect of capsaicin on claudin-3 distribution. Therefore, more efforts should be made to fully understand the effect of TRPV1 activation on each tight-junction component in salivary epithelium in various species and conditions.

We next explored the signaling pathway linking TRPV1 activation to occludin. Many studies revealed that MAPK activation in response to various factors is involved in modulation of tight junctions. Ouabain induces activation of ERK1/2, p38MAPK and JNK to cause redistribution of occludin, together with a concomitant drop in TER in MDCK cells (Contreras et al., 1999). In epithelial cells expressing constitutively active Ras or Raf-1, subsequent ERK1/2

activation causes a breakdown of tight junctions (Li and Mrsny, 2000). In acetaldehyde-treated Caco-2 cells, activation of ERK1/2, but not p38MAPK or JNK is involved in the EGF-mediated tight-junction disruption (Samak et al., 2011). These data indicated that MAPK plays an important role in the modulation of the tight-junction barrier in epithelia, but the specific member of MAPK family involved in the regulation of tight-junction function may vary in different cells and with different stimuli. In the present study, we found that TRPV1 activation by capsaicin increased phosphorylation of ERK1/2, but not p38MAPK and JNK, suggesting that ERK1/2 is the specific signaling target for TRPV1 in the conduction of intracellular signals. Furthermore, by using the ERK1/2 pharmacological inhibitor PD98059, as well as ERK1/2 siRNA, which showed higher inhibitory effectiveness than the inhibitor, the capsaicin-induced decrease in TER and occludin redistribution disappeared, further confirming that ERK1/2 plays a crucial role in the TRPV1-modulated paracellular permeability and occludin distribution.

Previous studies showed that tight-junction opening triggered by TNF- α , interferon (IFN)- γ or bile acids involves the phosphorylation of MLC2 (Zolotarevsky et al., 2002; Araki et al., 2005). In tubular epithelia, MLC2 is the downstream molecule modulated by ERK1/2, thereby mediating the TNF- α -induced increase in paracellular permeability (Kakiashvili et al., 2009; Waheed et al., 2010). In our present study, we found that the capsaicin-activated ERK1/2 could phosphorylate MLC2 and then affect the tight-junction barrier of SMG-C6 cells, indicating that MLC2 was also involved in the TRPV1-modulated tight-junction function.

The organization of the cytoskeletal F-actin contributes to tight-junction formation and function. MLC2 is considered to be one of the most common upstream kinases that regulate F-actin organization (Hecht et al., 1996; Bruewer et al., 2004; Shen et al., 2006). However, whether F-actin organization is involved in the TRPV1-modulated tight-junction barrier was unclear. We showed that TRPV1 activation caused reorganization of F-actin, and this effect was blocked by either PD98059 or ML-7, indicating that capsaicin induced F-actin reorganization in an ERK1/2- and MLC2-dependent manner. CytoB, a microfilament-disrupting agent, almost completely disrupted the expression of occludin at the membrane, which indicated that an intact F-actin organization was essential to maintain normal occludin distribution. Moreover, we observed that capsaicin-increased peripheral F-actin was reorganized very close to the cell-cell junctions. Therefore, we speculated that TRPV1-modulated F-actin organization might result in an enhanced interaction between F-actin and tight junctions and thereby drew one or some tight junction components into the cellular compartment followed by an opening of the paracellular transport.

In summary, we provided the first evidence that occludin not only plays a crucial role in regulating the tight-junction barrier of SMG-C6 cells, but is required for TRPV1-mediated increased paracellular permeability. We also showed that ERK1/2 signaling mediates TRPV1-modulated paracellular permeability and occludin distribution by activating the downstream MLC2 and reorganizing cytoskeletal F-actin. These findings will assist in further elucidating the significance of occludin in submandibular epithelial cells, and enriching our understanding of the mechanism involved in TRPV1-induced salivation.

Materials and Methods

Reagents and antibodies

Capsaicin, CPZ, Trypan Blue, PD98059, ML-7, CytoB, DMSO and FITC-labeled phalloidin were purchased from Sigma-Aldrich Co. (St Louis, MO, USA). The Ca^{2+} -sensitive indicator Fluo-3/AM was purchased from Biotium (Hayward, CA, USA). Antibodies to TRPV1, p-ERK1/2, ERK1/2, p-p38MAPK, p38MAPK, p-JNK, JNK, β -catenin, and actin were from Santa Cruz Biotechnology (Santa Cruz, CA, USA). Antibodies to occludin, Alexa-Fluor[®]-594-conjugated occludin, claudin-3 and claudin-4 were from Zymed/Invitrogen (Carlsbad, CA, USA). The antibody to E-cadherin was from Bioworld Technology (Minneapolis, MN, USA). Antibodies to p-MLC2 and MLC2 were from Cell Signaling Technology (Beverly, MA, USA).

Cell culture

The rat SMG cell line SMG-C6 (a kind gift from Dr David O. Quissell) was routinely grown at 37°C in a humidified 5% CO_2 atmosphere in DMEM/F12 (1:1 mixture) containing 2.5% fetal bovine serum, 5 $\mu\text{g}/\text{ml}$ transferrin, 1.1 $\mu\text{mol}/\text{l}$ hydrocortisone, 0.1 $\mu\text{mol}/\text{l}$ retinoic acid, 2 nmol/l thyronine T_3 , 5 $\mu\text{g}/\text{ml}$ insulin, 80 ng/ml epidermal growth factor, 50 $\mu\text{g}/\text{ml}$ gentamicin sulfate, 5 mmol/l glutamine, 100 U/ml penicillin and 100 $\mu\text{g}/\text{ml}$ streptomycin (Quissell et al., 1997). All constituents used in culturing SMG-C6 cells were purchased from Sigma-Aldrich Co. (St Louis, MO, USA).

Total RNA extraction and RT-PCR

Total RNA extraction and reverse transcription were performed as previously reported (Zhang et al., 2006). Briefly, total RNA was extracted with Trizol (Invitrogen, CA, USA) according to the manufacturer's instructions. cDNA was prepared from 4 μg of total RNA with M-MLV reverse transcriptase (Promega, WI, USA). The primer sequences for rat TRPV1 and tight-junction components are listed in supplementary material Table S1. The products were separated by electrophoresis on a 1.5% agarose gel, and DNA bands were visualized by staining with ethidium bromide.

Western blot analysis

The cultured cells were homogenized with lysis buffer (containing 50 mmol/l Tris-HCl, 150 mmol/l NaCl, 1 mmol/l EDTA, 1 mmol/l phenylmethylsulfonyl fluoride, 1% Triton X-100, 0.1% SDS, and 0.1% sodium deoxycholate, pH 7.2) using a polytron homogenizer as previously described (Shi et al., 2010). The homogenate was centrifuged at 1000 g for 10 min at 4°C, and the protein concentration of the supernatant was measured using the Bradford method. Equal amounts of proteins (40 μg) were separated using 9% SDS-PAGE and transferred to polyvinylidene difluoride membranes. The membranes were blocked with 5% non-fat milk for 1 hour at room temperature, probed with primary antibodies at 4°C overnight, and then incubated with horseradish-peroxidase-conjugated secondary antibodies. Immunoreactive bands were visualized with enhanced chemiluminescence (Pierce, IL, USA). The densities of bands were quantified with the ImageJ Software (National Institutes of Health, MD, USA). Actin was used as a loading control for standardization of blots.

Immunofluorescence staining

The SMG-C6 cells were plated on coverslips and fixed in 4% paraformaldehyde for 10 min. Following incubation with 1% BSA for 30 min at room temperature, the cells were stained with FITC-labeled phalloidin or FITC-labeled phalloidin plus Alexa-Fluor[®]-594-conjugated occludin for 2 hours at 37°C. The cells were also stained with antibodies for TRPV1, occludin, claudin-3, claudin-4, β -catenin or E-cadherin at 4°C overnight, and then incubated with Alexa-Fluor[®]-594-conjugated secondary antibodies (Molecular Probes, OR, USA), or Alexa-Fluor[®]-488-conjugated secondary antibodies plus Alexa-Fluor[®]-594-conjugated occludin for double staining, for 2 hours at 37°C. Fluorescence images were captured using a confocal microscope (Leica TCS SP5, Wetzlar, Germany).

Immunoprecipitation

The SMG-C6 cells were stimulated with 10 $\mu\text{mol}/\text{l}$ capsaicin for 10 min and total cell lysate was obtained. Immunoprecipitation was carried out by incubation with TRPV1 antibody and protein A/G beads overnight at 4°C. The beads were washed three times with lysis buffer and eluted with SDS-PAGE loading buffer. The proteins were separated using 9% SDS-PAGE and used for western blotting.

Preparation of cytoplasm and membrane fractions

Cytoplasm and membrane fractions were prepared as described previously (Kawedia et al., 2008). Briefly, cells were lysed in ice-cold 0.5% Triton X-100, 100 mM NaCl, 10 mM Tris-HCl (pH 7.4), and 300 mM sucrose for 20 min at 4°C. Then the detergent-soluble (cytoplasm fraction) protein was removed and the remaining insoluble residue was again lysed (membrane fraction) in 50 mM Tris (pH 6.8), 2% SDS and 10% glycerol.

TER measurement and non-selective monolayer permeability assay

Confluent monolayers of SMG-C6 cells were grown in 24-well Transwell[™] chambers (polycarbonate membrane, filter pore size: 0.4 μm ; filter area: 0.33 cm^2 ; Costar, USA) for 5–7 days. TER was measured at 37°C using an epithelial volt ohm meter (EVOM; WPI, FL, USA) as described previously (Turner et al., 1997). The background value of the blank filter (90 Ω) was subtracted, and all measurements were performed on a minimum of three wells. Trypan Blue was used as a paracellular tracer for non-selective monolayer permeability as performed previously (Sáenz-Morales et al., 2009; Strober, 2001). In brief, a cell monolayer was incubated for 15 min at 37°C with 0.04% Trypan Blue in the upper chamber. The amount of Trypan Blue contained in the medium of lower chamber was determined by spectrometry at 595 nm, and was represented as Trypan Blue influx rate ($\mu\text{g}/\text{min}$). The 4 kDa FITC-dextran was added apically, and samples were collected from the basal sides, 10 min after 10 $\mu\text{mol}/\text{l}$ capsaicin treatment. Using a fluorometer (BioTek, VT, USA), the apparent permeability coefficient (P_{app}) was calculated as the increase in the amount of tracer per time per filter area (Rosenthal et al., 2010).

Measurement of $[\text{Ca}^{2+}]_i$

The $[\text{Ca}^{2+}]_i$ was measured as previously described (Burchiel et al., 2000). Briefly, SMG-C6 cells were harvested from plates using trypsin, centrifuged, and resuspended in tubes at $\sim 10^6$ cells/200 μl in culture medium. Cells were loaded with the Ca^{2+} -sensitive fluorescent probe Fluo-3/AM (4 $\mu\text{mol}/\text{l}$) at 37°C in a CO_2 incubator for 60 min. After laser excitation at 488 nm the intensity of Fluo-3 fluorescence in the 30,000 harvested cells was analyzed on a FACSCalibur flow cytometer (BD Immunocytometry Systems, CA, USA). The traces shown are representative of at least three different cell preparations.

Knockdown of ERK1/2, occludin or claudin-3

SMG-C6 cells were cultured to 80% confluency and transfected with the siRNA or shRNA of interest using a MegeTran 1.0 (Origene, MD, USA) according to the manufacturer's instructions. The potent rat ERK1/2 siRNA sequence 5'-GACCGGAUGUUAACCUUUAUUt-3' and non-specific control were synthesized by GeneChem (Shanghai, China). For knockdown of occludin and claudin-3, shRNA constructs against rat occludin 5'-CTGTATTTCGCCTGCGTG-GCTTCCACACTT-3', claudin-3 5'-CTCTCATCGTGGTGTCTATCCTACTGG-CA-3' and scrambled control were constructed in pGFP-V-RS vectors and synthesized by Origene Technologies (Origene, MD, USA). The cells were collected or fixed at least 24 hours after transfection.

Re-expression of occludin

Occludin re-expression ('rescue') was performed by generating a GFP-tagged cDNA clone of occludin in a pCMV6 vector (Origene, MD, USA). Plasmid transfection was carried out with MegeTran 1.0 (Origene, MD, USA) and the ratio of transfection reagent to DNA was 3:1 as described in the manufacturer's instructions. At 24 hours post-transfection, the cells were collected or used for experiments.

Statistical analysis

Data are presented as means \pm s.d. Statistical analyses between multiple groups were performed by one-way ANOVA and followed by Bonferroni's test using GraphPad software (GraphPad Prism, CA, USA). $P < 0.05$ was considered significant.

Acknowledgements

We thank Dr David O. Quissell from the School of Dentistry, University of Colorado Health Sciences Center, Denver, CO, USA, for the generous gift of rat SMG-C6 cell line.

Author contributions

G.Y. Yu, L.L. Wu., X. Cong and Y. Zhang designed the project; X. Cong, N.Y. Yang, J. Li, C. Ding, Q.W., Ding, Y.C. Su performed experiments; M. Mei and X.H. Guo contributed to statistical analysis; G.Y. Yu, L.L. Wu, X. Cong and Y. Zhang contributed to writing of the manuscript.

Funding

This study was supported by the National Science Foundation of China [grant numbers 81070847 to G.Y., 30730102 to G.Y., 81271161 to G.Y. and 81170974 to Y.Z.].

Supplementary material available online at

<http://jcs.biologists.org/lookup/suppl/doi:10.1242/jcs.111781/-/DC1>

References

- Akiba, Y., Kato, S., Katsube, K., Nakamura, M., Takeuchi, K., Ishii, H. and Hibi, T. (2004). Transient receptor potential vanilloid subfamily 1 expressed in pancreatic islet beta cells modulates insulin secretion in rats. *Biochem. Biophys. Res. Commun.* **321**, 219-225.
- Anderson, J. M. and Van Itallie, C. M. (2009). Physiology and function of the tight junction. *Cold Spring Harb. Perspect. Biol.* **1**, a002584.
- Araki, Y., Katoh, T., Ogawa, A., Bamba, S., Andoh, A., Koyama, S., Fujiyama, Y. and Bamba, T. (2005). Bile acid modulates transepithelial permeability via the generation of reactive oxygen species in the Caco-2 cell line. *Free Radic. Biol. Med.* **39**, 769-780.
- Auzanneau, C., Norez, C., Antigny, F., Thoreau, V., Jouglu, C., Cantereau, A., Becq, F. and Vandebrouck, C. (2008). Transient receptor potential vanilloid 1 (TRPV1) channels in cultured rat Sertoli cells regulate an acid sensing chloride channel. *Biochem. Pharmacol.* **75**, 476-483.
- Balda, M. S., Whitney, J. A., Flores, C., González, S., Cerejido, M. and Matter, K. (1996). Functional dissociation of paracellular permeability and transepithelial electrical resistance and disruption of the apical-basolateral intramembrane diffusion barrier by expression of a mutant tight junction membrane protein. *J. Cell Biol.* **134**, 1031-1049.
- Balda, M. S., Flores-Maldonado, C., Cerejido, M. and Matter, K. (2000). Multiple domains of occludin are involved in the regulation of paracellular permeability. *J. Cell. Biochem.* **78**, 85-96.
- Bamforth, S. D., Kniesel, U., Wolburg, H., Engelhardt, B. and Risau, W. (1999). A dominant mutant of occludin disrupts tight junction structure and function. *J. Cell Sci.* **112**, 1879-1888.
- Bengtsson, T., Jaconi, M. E., Gustafson, M., Magnusson, K. E., Theler, J. M., Lew, D. P. and Stendahl, O. (1993). Actin dynamics in human neutrophils during adhesion and phagocytosis is controlled by changes in intracellular free calcium. *Eur. J. Cell Biol.* **62**, 49-58.
- Birder, L. A., Kanai, A. J., de Groat, W. C., Kiss, S., Nealen, M. L., Burke, N. E., Dineley, K. E., Watkins, S., Reynolds, I. J. and Caterina, M. J. (2001). Vanilloid receptor expression suggests a sensory role for urinary bladder epithelial cells. *Proc. Natl. Acad. Sci. USA* **98**, 13396-13401.
- Bruewer, M., Hopkins, A. M., Hobert, M. E., Nusrat, A. and Madara, J. L. (2004). RhoA, Rac1, and Cdc42 exert distinct effects on epithelial barrier via selective structural and biochemical modulation of junctional proteins and F-actin. *Am. J. Physiol. Cell Physiol.* **287**, C327-C335.
- Burchiel, S. W., Edwards, B. S., Kuckuck, F. W., Lauer, F. T., Prossnitz, E. R., Ransom, J. T. and Sklar, L. A. (2000). Analysis of free intracellular calcium by flow cytometry: multiparameter and pharmacologic applications. *Methods* **21**, 221-230.
- Caterina, M. J., Schumacher, M. A., Tominaga, M., Rosen, T. A., Levine, J. D. and Julius, D. (1997). The capsaicin receptor: a heat-activated ion channel in the pain pathway. *Nature* **389**, 816-824.
- Cong, X., Zhang, Y., Shi, L., Yang, N. Y., Ding, C., Li, J., Ding, Q. W., Su, Y. C., Xiang, R. L., Wu, L. L. et al. (2012). Activation of transient receptor potential vanilloid subtype 1 increases expression and permeability of tight junction in normal and hyposecretory submandibular gland. *Lab. Invest.* **92**, 753-768.
- Contreras, R. G., Shoshani, L., Flores-Maldonado, C., Lázaro, A. and Cerejido, M. (1999). Relationship between Na(+),K(+)-ATPase and cell attachment. *J. Cell Sci.* **112**, 4223-4232.
- Coyne, C. B., Shen, L., Turner, J. R. and Bergelson, J. M. (2007). Coxsackievirus entry across epithelial tight junctions requires occludin and the small GTPases Rab34 and Rab5. *Cell Host Microbe* **2**, 181-192.
- Ding, Q. W., Zhang, Y., Wang, Y., Wang, Y. N., Zhang, L., Ding, C., Wu, L. L. and Yu, G. Y. (2010). Functional vanilloid receptor-1 in human submandibular glands. *J. Dent. Res.* **89**, 711-716.
- Ewert, P., Aguilera, S., Allende, C., Kwon, Y. J., Albornoz, A., Molina, C., Urzúa, U., Quest, A. F., Olea, N., Pérez, P. et al. (2010). Disruption of tight junction structure in salivary glands from Sjögren's syndrome patients is linked to proinflammatory cytokine exposure. *Arthritis Rheum.* **62**, 1280-1289.
- Furuse, M., Hirase, T., Itoh, M., Nagafuchi, A., Yonemura, S., Tsukita, S. and Tsukita, S. (1993). Occludin: a novel integral membrane protein localizing at tight junctions. *J. Cell Biol.* **123**, 1777-1788.
- González-Mariscal, L., Tapia, R. and Chamorro, D. (2008). Crosstalk of tight junction components with signaling pathways. *Biochim. Biophys. Acta* **1778**, 729-756.
- Hashimoto, S. and Murakami, M. (2009). Morphological evidence of paracellular transport in perfused rat submandibular glands. *J. Med. Invest.* **56 Suppl.**, 395-397.
- Hecht, G., Pestic, L., Nikcevic, G., Koutsouris, A., Tripuraneni, J., Lorimer, D. D., Nowak, G., Guerriero, V., Jr, Elson, E. L. and Lanerolle, P. D. (1996). Expression of the catalytic domain of myosin light chain kinase increases paracellular permeability. *Am. J. Physiol.* **271**, C1678-C1684.
- Hou, J., Renigunta, A., Yang, J. and Waldegger, S. (2010). Claudin-4 forms paracellular chloride channel in the kidney and requires claudin-8 for tight junction localization. *Proc. Natl. Acad. Sci. USA* **107**, 18010-18015.
- Inoue, K., Koizumi, S., Fuziwara, S., Denda, S., Inoue, K. and Denda, M. (2002). Functional vanilloid receptors in cultured normal human epidermal keratinocytes. *Biochem. Biophys. Res. Commun.* **291**, 124-129.
- Isoda, H., Han, J., Tominaga, M. and Maekawa, T. (2001). Effects of capsaicin on human intestinal cell line Caco-2. *Cytotechnology* **36**, 155-161.
- Kakiashvili, E., Speight, P., Waheed, F., Seth, R., Lodyga, M., Tanimura, S., Kohno, M., Rotstein, O. D., Kapus, A. and Szász, K. (2009). GEF-H1 mediates tumor necrosis factor-alpha-induced Rho activation and myosin phosphorylation: role in the regulation of tubular paracellular permeability. *J. Biol. Chem.* **284**, 11454-11466.
- Kawedia, J. D., Nieman, M. L., Boivin, G. P., Melvin, J. E., Kikuchi, K., Hand, A. R., Lorenz, J. N. and Menon, A. G. (2007). Interaction between transcellular and paracellular water transport pathways through Aquaporin 5 and the tight junction complex. *Proc. Natl. Acad. Sci. USA* **104**, 3621-3626.
- Kawedia, J. D., Jiang, M., Kulkarni, A., Waechter, H. E., Matlin, K. S., Pauletti, G. M. and Menon, A. G. (2008). The protein kinase A pathway contributes to Hg2+-induced alterations in phosphorylation and subcellular distribution of occludin associated with increased tight junction permeability of salivary epithelial cell monolayers. *J. Pharmacol. Exp. Ther.* **326**, 829-837.
- Lee, M. G., Macglashan, D. W., Jr and Undem, B. J. (2005). Role of chloride channels in bradykinin-induced guinea pig airway vagal C-fibre activation. *J. Physiol.* **566**, 205-212.
- Li, D. and Mrsny, R. J. (2000). Oncogenic Raf-1 disrupts epithelial tight junctions via downregulation of occludin. *J. Cell Biol.* **148**, 791-800.
- Liu, S., Yang, W., Shen, L., Turner, J. R., Coyne, C. B. and Wang, T. (2009). Tight junction proteins claudin-1 and occludin control hepatitis C virus entry and are downregulated during infection to prevent superinfection. *J. Virol.* **83**, 2011-2014.
- Lourenço, S. V., Coutinho-Camillo, C. M., Buim, M. E., Uyekita, S. H. and Soares, F. A. (2007). Human salivary gland branching morphogenesis: morphological localization of claudins and its parallel relation with developmental stages revealed by expression of cytoskeleton and secretion markers. *Histochem. Cell Biol.* **128**, 361-369.
- Marchiando, A. M., Shen, L., Graham, W. V., Weber, C. R., Schwarz, B. T., Austin, J. R., 2nd, Raleigh, D. R., Guan, Y., Watson, A. J., Montrose, M. H. et al. (2010). Caveolin-1-dependent occludin endocytosis is required for TNF-induced tight junction regulation in vivo. *J. Cell Biol.* **189**, 111-126.
- McCarthy, K. M., Skare, I. B., Stankewich, M. C., Furuse, M., Tsukita, S., Rogers, R. A., Lynch, R. D. and Schneeberger, E. E. (1996). Occludin is a functional component of the tight junction. *J. Cell Sci.* **109**, 2287-2298.
- Murakami, M., Shachar-Hill, B., Steward, M. C. and Hill, A. E. (2001). The paracellular component of water flow in the rat submandibular salivary gland. *J. Physiol.* **537**, 899-906.
- Musch, M. W., Walsh-Reitz, M. M. and Chang, E. B. (2006). Roles of ZO-1, occludin, and actin in oxidant-induced barrier disruption. *Am. J. Physiol. Gastrointest. Liver Physiol.* **290**, G222-G231.
- Nybo, P. and Magnusson, K. E. (1996). Modulation of the junctional integrity by low or high concentrations of cytochalasin B and dihydrocytochalasin B is associated with distinct changes in F-actin and ZO-1. *Biosci. Rep.* **16**, 313-326.
- Peixoto, E. B. and Collares-Buzato, C. B. (2005). Protamine-induced epithelial barrier disruption involves rearrangement of cytoskeleton and decreased tight junction-associated protein expression in cultured MDCK strains. *Cell Struct. Funct.* **29**, 165-178.
- Peppi, M. and Ghabriel, M. N. (2004). Tissue-specific expression of the tight junction proteins claudins and occludin in the rat salivary glands. *J. Anat.* **205**, 257-266.
- Quissell, D. O., Barzen, K. A., Gruenert, D. C., Redman, R. S., Camden, J. M. and Turner, J. T. (1997). Development and characterization of SV40 immortalized rat submandibular acinar cell lines. *In Vitro Cell. Dev. Biol. Anim.* **33**, 164-173.
- Reiter, B., Kraft, R., Günzel, D., Zeissig, S., Schulzke, J. D., Fromm, M. and Harteneck, C. (2006). TRPV4-mediated regulation of epithelial permeability. *FASEB J.* **20**, 1802-1812.
- Rosenthal, R., Milatz, S., Krug, S. M., Oelrich, B., Schulzke, J. D., Amasheh, S., Günzel, D. and Fromm, M. (2010). Claudin-2, a component of the tight junction, forms a paracellular water channel. *J. Cell Sci.* **123**, 1913-1921.
- Sáenz-Morales, D., Conde, E., Escribese, M. M., García-Martos, M., Alegre, L., Blanco-Sánchez, I. and García-Bermejo, M. L. (2009). ERK1/2 mediates cytoskeleton and focal adhesion impairment in proximal epithelial cells after renal ischemia. *Cell. Physiol. Biochem.* **23**, 285-294.
- Saitou, M., Fujimoto, K., Doi, Y., Itoh, M., Fujimoto, T., Furuse, M., Takano, H., Noda, T. and Tsukita, S. (1998). Occludin-deficient embryonic stem cells can differentiate into polarized epithelial cells bearing tight junctions. *J. Cell Biol.* **141**, 397-408.
- Saitou, M., Furuse, M., Sasaki, H., Schulzke, J. D., Fromm, M., Takano, H., Noda, T. and Tsukita, S. (2000). Complex phenotype of mice lacking occludin, a component of tight junction strands. *Mol. Biol. Cell* **11**, 4131-4142.
- Samak, G., Aggarwal, S. and Rao, R. K. (2011). ERK is involved in EGF-mediated protection of tight junctions, but not adherens junctions, in acetaldehyde-treated Caco-2 cell monolayers. *Am. J. Physiol. Gastrointest. Liver Physiol.* **301**, G50-G59.
- Saunders, C. I., Kunde, D. A., Crawford, A. and Geraghty, D. P. (2007). Expression of transient receptor potential vanilloid 1 (TRPV1) and 2 (TRPV2) in human peripheral blood. *Mol. Immunol.* **44**, 1429-1435.
- Schaphorst, K. L., Chiang, E., Jacobs, K. N., Zaiman, A., Natarajan, V., Wigley, F. and Garcia, J. G. (2003). Role of sphingosine-1 phosphate in the enhancement of endothelial barrier integrity by platelet-released products. *Am. J. Physiol. Lung Cell. Mol. Physiol.* **285**, L258-L267.
- Segawa, A. (1994). Tight junctional permeability in living cells: dynamic changes directly visualized by confocal laser microscopy. *J. Electron Microsc. (Tokyo)* **43**, 290-298.
- Shen, L., Black, E. D., Witkowski, E. D., Lencer, W. I., Guerriero, V., Schneeberger, E. E. and Turner, J. R. (2006). Myosin light chain phosphorylation regulates barrier function by remodeling tight junction structure. *J. Cell Sci.* **119**, 2095-2106.

- Shi, L., Cong, X., Zhang, Y., Ding, C., Ding, Q. W., Fu, F. Y., Wu, L. L. and Yu, G. Y. (2010). Carbachol improves secretion in the early phase after rabbit submandibular gland transplantation. *Oral Dis.* **16**, 351-359.
- Shifflett, D. E., Clayburgh, D. R., Koutsouris, A., Turner, J. R. and Hecht, G. A. (2005). Enteropathogenic *E. coli* disrupts tight junction barrier function and structure in vivo. *Lab. Invest.* **85**, 1308-1324.
- Strober, W. (2001). Trypan blue exclusion test of cell viability. *Curr. Protoc. Immunol.* **21**, A.3B.1-A.3B.2.
- Tsukita, S., Furuse, M. and Itoh, M. (2001). Multifunctional strands in tight junctions. *Nat. Rev. Mol. Cell Biol.* **2**, 285-293.
- Tunggal, J. A., Helfrich, I., Schmitz, A., Schwarz, H., Günzel, D., Fromm, M., Kemler, R., Krieg, T. and Niessen, C. M. (2005). E-cadherin is essential for in vivo epidermal barrier function by regulating tight junctions. *EMBO J.* **24**, 1146-1156.
- Turner, J. R., Rill, B. K., Carlson, S. L., Carnes, D., Kerner, R., Mrsny, R. J. and Madara, J. L. (1997). Physiological regulation of epithelial tight junctions is associated with myosin light-chain phosphorylation. *Am. J. Physiol.* **273**, C1378-C1385.
- Van Itallie, C. M., Fanning, A. S., Holmes, J. and Anderson, J. M. (2010). Occludin is required for cytokine-induced regulation of tight junction barriers. *J. Cell Sci.* **123**, 2844-2852.
- Veronesi, B., Carter, J. D., Devlin, R. B., Simon, S. A. and Oortgiesen, M. (1999). Neuropeptides and capsaicin stimulate the release of inflammatory cytokines in a human bronchial epithelial cell line. *Neuropeptides* **33**, 447-456.
- Waheed, F., Speight, P., Kawai, G., Dan, Q., Kapus, A. and Szász, K. (2010). Extracellular signal-regulated kinase and GEF-H1 mediate depolarization-induced Rho activation and paracellular permeability increase. *Am. J. Physiol. Cell Physiol.* **289**, C1376-C1387.
- Yu, D. and Turner, J. R. (2008). Stimulus-induced reorganization of tight junction structure: the role of membrane traffic. *Biochim. Biophys. Acta* **1778**, 709-716.
- Zhang, Y., Xiang, B., Li, Y. M., Wang, Y., Wang, X., Wang, Y. N., Wu, L. L. and Yu, G. Y. (2006). Expression and characteristics of vanilloid receptor 1 in the rabbit submandibular gland. *Biochem. Biophys. Res. Commun.* **345**, 467-473.
- Zolotarevsky, Y., Hecht, G., Koutsouris, A., Gonzalez, D. E., Quan, C., Tom, J., Mrsny, R. J. and Turner, J. R. (2002). A membrane-permeant peptide that inhibits MLC kinase restores barrier function in in vitro models of intestinal disease. *Gastroenterology* **123**, 163-172.